RSC Advances

ROYAL SOCIETY OF CHEMISTRY

PAPER

Cite this: *RSC Adv.*, 2015, **5**, 54843

HPSTAR 0106-2015

Anomalous semiconducting behavior on VO_2 under high pressure

Xin Zhang,[a] Junkai Zhang,[b] Feng Ke,[b] Guanghui Li,[a] Yanmei Ma,[a] Xizhe Liu,[a] Cailong Liu,*[a] Yonghao Han,[a] Yanzhang Ma[c] and Chunxiao Gao*[a]

Received 28th April 2015
Accepted 17th June 2015

DOI: 10.1039/c5ra07732j

www.rsc.org/advances

High-pressure electrical transport properties of VO_2 have been investigated by *in situ* resistivity, Hall-effect, and temperature dependence of resistivity measurements. The electrical transport parameters including resistivity, Hall coefficient, carrier concentration, and mobility varies significantly around 10.4 GPa, which can be attributed to the isostructural phase transition of VO_2. Temperature dependence of resistivity indicates that the phase transition is a semiconductor-to-semiconductor transformation, not the pressure-induced metallization as previously reported by Raman and IR experiment observations. The dramatic increase of activation energy at 10.4 GPa indicates an increasingly insulating behavior of VO_2 accompanied with the isostructural phase transition. The electrical transport properties, especially the carries transportation under compression open up a new possible basis for optimizing the performance of VO_2 based applications under ambient or extreme conditions.

1. Introduction

The transition metal oxide VO_2 has attracted considerable interest because of its temperature-induced sharp variation on resistivity and dramatic alteration in optical reflectance. In 1959, F. J. Morin *et al.* firstly reported that VO_2 underwent an insulator-metal transition (IMT) accompanied by a sharp reduction in resistance by about several orders of magnitude at $T \approx 340$ K.[1]

Then, the V–V pairing and electron correlation were found to play an important role on driving the system from a slightly less correlated insulator ($T < 340$ K) to a correlated metal ($T > 340$ K).[2–4] And during the IMT, the optical properties of VO_2 in the infrared region were drastically changed in reflectance from 2 to 94%.[5–7] The IMT was also reported to be a first-order structural phase transition from insulating monoclinic phase (space group $P2_1/c$)[8–17] to metallic tetragonal phase (space group $P4_2/mnm$).[8]

Compression is an effective approach to explore new materials and new phases. Pressure can also modulate the conducting behavior of material, for instance, the single metal Na transforms into insulating state and the semiconductor Bi_2Te_3 transforms into metallic state under compression.[18,19] It is a meaningful project to verify whether VO_2 undergoes the pressure-induced semiconductor-to-metal transformation, just like the IMT. In 1969, C. Berglund *et al.* proposed that applying compression can affect the critical temperature of the IMT on VO_2, and the transition temperature increases with increasing pressure with a rate of (82 ± 5) mK kbar^{-1}.[20] In 2007, E. Arcangeletti *et al.* indicate that pressure can drive the semiconductor-to-metal transformation of VO_2 at 10 GPa.[21,22] In 2012, M. Mitrano *et al.* used the X-ray powder diffraction measurements to indicate that VO_2 has an isostructural phase transition at about 12.0 GPa.[23] At this isostructural phase transition, pressure drivers a slight rearrangement of the V chains leading to a common monoclinic phase and a significant anisotropy in lattice compression of the *b* and *c* plane.[22,23] At present, few study can be found about the pressure-induced metallization on VO_2 under compression. We require more direct and effective measurements to prove the metallization of VO_2 at certain pressures.

In this work, we carried out accurate *in situ* resistivity, Hall-effect, and temperature dependence of resistivity measurements to verify whether or not VO_2 undergoes the phase transition and a semiconductor-to-metal transformation under compression, and observed the comprehensive electrical transport behavior of charge carriers to provide new guidance for its practical application.

[a]State Key Lab of Superhard Materials, Institute of Atomic and Molecular, Jilin University, Changchun 130012, China. E-mail: cailong_liu@jlu.edu.cn; cc060109@qq.com
[b]Center for High Pressure Science and Technology Advanced Research, Shanghai 201203, China
[c]Department of Mechanical Engineering, Texas Tech University, Lubbock, TX79409, USA

2. Experimental methods

High-pressure experiments were carried out using a nonmagnetic diamond anvil cell (DAC) with an anvil culet of 400 μm in diameter. A nonmagnetic rhenium flake was indented to a thickness of 50 μm served as gasket. A hole with 150 μm in

This journal is © The Royal Society of Chemistry 2015

diameter was drilled in the center of the indentation served as a sample chamber, and alumina film with thickness of 2 μm was sputtered on the gasket for insulation. To measure the electrical parameters accurately, the hole was fully covered with sample. And no pressure transmitting medium was used in order to avoid the introduction of impurities. The sample thickness under pressure was determined by a micrometer with a precision of 0.5 μm, and the deformation of diamond anvils was taken into account.[24] Pressure was determined using the ruby fluorescence method. Polycrystalline VO_2 powder brought from Alfa Aesar Co. with a stated purity of 99% was used as the sample.

van der Pauw configuration film microcircuit was integrated on a diamond surface. The fabricating method of the Mo film electrodes has been reported previously,[25,26] as shown in Fig. 1. The resistivity of the sample was determined by the van der Pauw method[27] with the following formula,

$$\exp(-\pi d R_a/\rho) + \exp(-\pi d R_b/\rho) = 1 \tag{1}$$

where ρ and d are the resistivity and the thickness of the sample, respectively; R_a and R_b are electrical resistance with $R_a = V_{DC}/I_{AB}$ and $R_b = V_{AD}/I_{BC}$. During the measurement, a 10 μA current I_{AB} was introduced through applied by electrodes A and B, meanwhile the voltage drop V_{DC} was measured. The same measurement process was conducted round in all electrodes. The detailed measurement and calculation methods have been reported previously.

During the *in situ* Hall-effect measurement under high pressure, a lakeshore Gauss meter (model 420) was employed to monitor the magnetic flux density by putting the meter probe near the sample. And the current reversal method was used to avoid thermoelectric offsets. The electrical current I was supplied by a Keithley 2400 current source, and the voltage V_H was measured by a Keithley 2700 multimeter. The magnetic flux density B applied to the sample was 1.0 T in the Hall-effect measurements. All instruments were connected to a computer *via* a Keithley Kusb-488 interface adapter and a general purpose interface bus. The Hall coefficient R_H was calculated by the equation, $R_H = V_H d/IB$, and the Hall carrier concentration n was determined from the Hall coefficient using $n = 1/(R_H e)$ relation, where e is the electron change. The Hall mobility μ was obtained from the zero-field electrical resistivity and Hall coefficient $\mu = R_H/\rho$. The measurement process was automatically performed according to the van der Pauw method.

For temperature dependence of resistivity measurements, the low temperature condition was obtained by liquid nitrogen, and measured by a K-type thermocouple which was glued onto the side of diamond. The electrical current was also provided by a Keithley 2400 current source, and the voltage drop was measured by a Keithley 2700 multimeter.

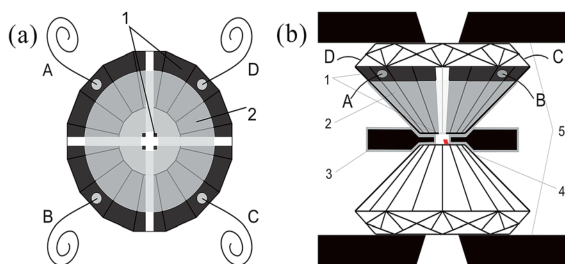

Fig. 1 (a) Configuration of a microcircuit on a diamond anvil: 1 is Mo electrode, 2 is the alumina layer, and A–D are the lead wires. (b) The cross section of the diamond anvil cell device. Here 3 is the gasket, 4 is the ruby, 5 is the pedestal, and 1, 2, and A–D correspond to those in (a).

3. Results and discussion

3.1 *In situ* resistivity measurements under high pressure

Shown in Fig. 2 is pressure dependence of resistivity of sample at room temperature. At ambient pressure, the resistivity of sample is 0.87 Ω cm. Under high pressure, the resistivity of VO_2 decreases more than 2 orders of magnitude. From ambient to 10.4 GPa, the resistivity decreases smoothly with increasing pressure. Above 10.4 GPa, it turns to be decreasing more quickly. A significant inflection point of the resistivity appears at this pressure, consistent with previously reported pressure-induced isostructural phase transition of VO_2.[21–23,28]

During the decompression process, the inflection point of resistivity appears around 8.8 GPa. After the full pressure releasing, resistivity of VO_2 returns to its original value. Hence we infer that the phase transition of VO_2 have a big possibility to be reversible.[29,30] However, *in situ* XRD experiments should be done to give direct evidence in the future.

3.2 Temperature dependence of resistivity measurements

To determine whether or not VO_2 undergoes a semiconductor-to-metal transformation under pressure, the temperature dependence of resistivity measurement was carried out between 90 and 270 K at representative pressures, as shown in Fig. 3. In the whole pressure range, the temperature coefficients of VO_2 are negative ($d\rho/dT < 0$), which indicates that VO_2 always shows the semiconductor behavior under pressure.

Based on the Arrhenius equation

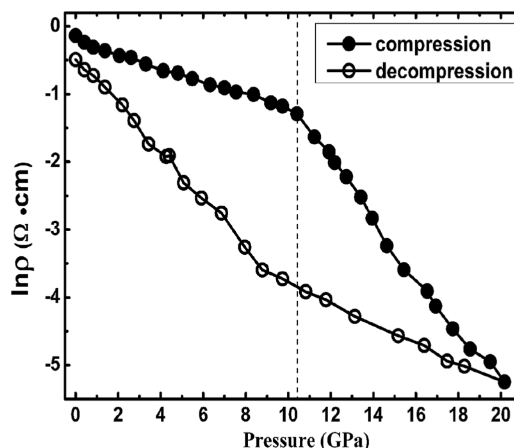

Fig. 2 Pressure dependence of electrical resistivity of sample at room temperature. The vertical dashed line indicates the phase transition.

 This journal is © The Royal Society of Chemistry 2015

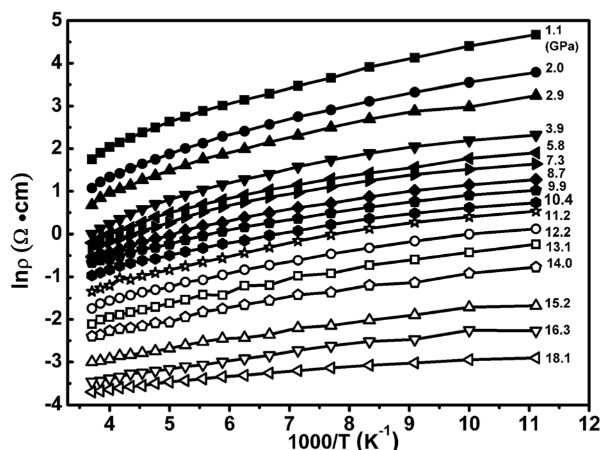

Fig. 3 Temperature dependence resistivity of VO_2 plotted in Arrhenius format at representative pressures in the range 90 K < T < 270 K.

$$\rho = \rho_0 \exp(-E_t/2k_BT) \quad (2)$$

where ρ_0 is high temperature resistivity, ρ is the electrical resistivity, k_B is Boltzmann constant, T is the temperature, and E_t is the transport activation energy of the carrier, we obtain $E_t = 2k_B\partial \ln \rho/\partial(1/T)$. And E_t can be obtained by linearly fitting the plots of ln ρ *vs.* 1000/T, as shown in Fig. 4. Below 10.4 GPa, E_t decreases monotonously with increasing pressure with a rate of $\sim$−15.6 meV GPa^{-1}. For VO_2, E_t is determined by the donors energy levels provided by O vacancies.[31] The negative slope of E_t *vs.* P curve indicates that the donors energy levels move toward π bands (conduction band) of V atoms and the energy gap decreases with increasing pressure, which reduces the energy barriers height and makes carriers transport easier. And the phase transition can induce the jump of E_t at about 10.4 GPa as shown in shadow part of Fig. 4, which indicates an increasingly insulating behavior of VO_2 during the phase transition. Above 10.4 GPa, E_t decreases with increasing pressure at a rate of $\sim$−25.1 meV GPa^{-1}. And in the whole pressure range, the changes of E_t with the pressure is well consistent with the change results of resistivity of sample.

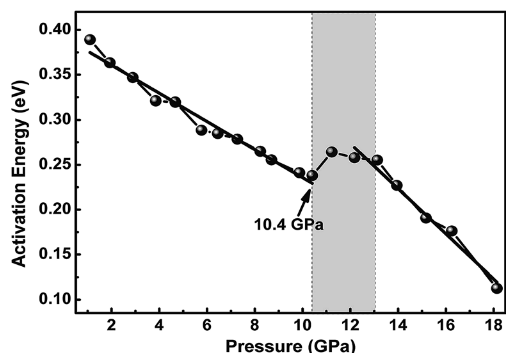

Fig. 4 Pressure dependence of the carrier transport activation energy of VO_2 obtained by fitting the temperature dependence of resistivity.

3.3 *In situ* Hall-effect measurements under high pressure

To gain further insight into the carriers transport properties of VO_2, we performed *in situ* Hall-effect measurement under pressure. Fig. 5 shows the pressure dependence of Hall coefficient (R_H), carrier concentration (n), and mobility (μ) under magnetic field of 1.0 T. At ambient pressure, R_H, n, and μ of VO_2 are 0.4 cm^3 C^{-1}, 1.6 × 10^{19} cm^{-3}, and 0.5 cm^2 V^{-1} s^{-1} respectively. All electrical transport parameters display discontinuous changes at about 10.4 GPa. The value of R_H is negative in the whole pressure range, which indicates the electron carrier is always the major dominate carrier under pressure.

Before 10.4 GPa, R_H, n and μ increasing with increasing pressure. n of VO_2 is mainly determined by the donor energy levels related with the activation energy. From the equation $n \propto e^{-E_t/2kT}$ (3), the decrease in the activation energy E_t (as shown in Fig. 4) indicates pressure can drive electron carriers transferring easier to the bottom of conduction band. Thus the electron concentration increases under pressure. On the other hand, μ increases slowly before 10.4 GPa. The above indicates that the decreasing of the resistivity with increasing pressure up to 10.4 GPa is due to the both contribution of electron concentration and mobility.

At about 10.4 GPa, the carrier concentration shows an inconspicuous jump. Herein this inflexion point corresponds to

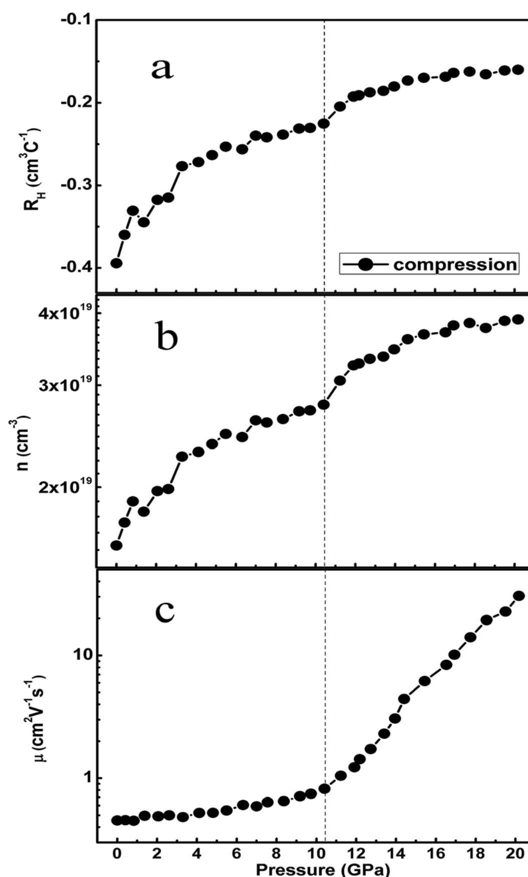

Fig. 5 Pressure dependences of Hall coefficient, carrier concentration, and mobility of VO_2 at room temperature.

This journal is © The Royal Society of Chemistry 2015

the phase transition of the V–V dimmers rearrange as reported by E. Arcangeletti.[21] In addition, μ also shows an obvious inflexion at this pressure. And the increasing rate of electron mobility shows obvious changes before and after 10.4 GPa. According to the $k \cdot p$ model, the increase of the electron mobility is likely to be mainly determined by the decrease of the electron effective mass, correlated with the decreasing of the band gap.[32] For the ionized impurity scattering, the electron effective mass decreases with the decreasing of band gap, which contributes to the increase in the electron mobility. Moreover, intervals between grains decrease with increasing of the pressure. This may weaken scattering of grain boundary and cause of the increase of μ in all pressure ranges.[33] Furthermore, electron mobility increases less than 1 $cm^2 V^{-1} s^{-1}$ from 0 GPa to 10.4 GPa, but increases near 10 $cm^2 V^{-1} s^{-1}$ from 10.4 GPa to 20.2 GPa. The rapid increase in the electron mobility is the dominant effect producing the decrease in ρ between 10.4 GPa and 20.2 GPa as shown in Fig. 2.

4. Conclusions

In this work, we have carried out the accurate *in situ* resistivity, Hall-effect, and temperature dependent resistivity measurements on VO_2 up to 20.2 GPa. The isostructural phase transition, gives rise to the discontinuous changes of resistivity, Hall coefficient, carrier concentration, and mobility. The results of Hall coefficient indicate that the electron carriers are dominant in the conducting progress. Furthermore, the change of electrical resistivity with the temperature shows that VO_2 always displays the semiconductor characterization before and after the phase transition.

Acknowledgements

This work was supported by the National Basic Research Program of China (Grant no. 2011CB808204), the National Natural Science Foundation of China (Grant nos, 11374121, 11404133, 11304114, and 51273079), and the Program of Science and Technology Development Plan of Jilin Province (Grant no. 20140520105JH).

References

1 F. J. Morin, *Phys. Rev. Lett.*, 1959, **3**, 34.
2 K. L. Holman, T. M. McQueen, A. J. Williams, T. Klimczuk, P. W. Stephens, H. W. Zandbergen, Q. Xu, F. Ronning and R. J. Cava, *Phys. Rev. B: Condens. Matter Mater. Phys.*, 2009, **79**, 245114.
3 M. Imada, A. Fujimori and Y. Tokura, *Rev. Mod. Phys.*, 1998, **70**, 1039.
4 J. Tomczak, F. Aryasetiawan and S. Biermann, *Phys. Rev. B: Condens. Matter Mater. Phys.*, 2008, **78**, 115103.
5 H. S. Choi, J. S. Ahn, J. H. Jung, T. W. Noh and D. H. Kim, *Phys. Rev. B: Condens. Matter Mater. Phys.*, 1996, **54**, 4621.
6 D. Ruzmetov, K. T. Zawilski, S. D. Senanayake, V. Narayanamurti and S. Ramanathan, *J. Phys.: Condens. Matter*, 2008, **20**, 465204.
7 M. M. Qazilbash, Z. Q. Li, V. Podzorov, M. Brehm, F. Keilmann, B. G. Chae, H. T. Kim and D. N. Basov, *Appl. Phys. Lett.*, 2008, **92**, 241906.
8 D. McWhan, M. Marezio, J. Remeika and P. Dernier, *Phys. Rev. B: Condens. Matter Mater. Phys.*, 1974, **10**, 490.
9 J. M. Longo and P. Kierkegaard, *Acta Chem. Scand.*, 1970, **24**, 7.
10 M. Hada, K. Okimura and J. Matsuo, *Phys. Rev. B: Condens. Matter Mater. Phys.*, 2010, **82**, 153401.
11 J. B. Goodenough, *J. Solid State Chem.*, 1971, **3**, 490.
12 L. A. Ladd and W. Paul, *Solid State Commun.*, 1969, **7**, 425.
13 S. Shin, S. Suga, M. Taniguchi, M. Fujisawa, H. Kanzaki, A. Fujimori, H. Daimon, Y. Ueda, K. Kosuge and S. Kachi, *Phys. Rev. B: Condens. Matter Mater. Phys.*, 1990, **41**, 4993.
14 H. W. Verleur, A. S. Barker, Jr. and C. N. Berglund, *Phys. Rev.*, 1968, **172**, 788.
15 S. Biermann, A. Poteryaev, A. Lichtenstein and A. Georges, *Phys. Rev. Lett.*, 2005, **94**, 026404.
16 M. W. Haverkort, Z. Hu, A. Tanaka, W. Reichelt, S. V. Streltsov, M. A. Korotin, V. I. Anisimov, H. H. Hsieh, H.-J. Lin, C. T. Chen, D. I. Khomskii and L. H. Tjeng, *Phys. Rev. Lett.*, 2005, **95**, 196404.
17 K. Okazaki, H. Wadati, A. Fujimori, M. Onoda, Y. Muraoka and Z. Hiroi, *Phys. Rev. B: Condens. Matter Mater. Phys.*, 2004, **69**, 165104.
18 Y. Ma, M. Eremets, A. R. Oganov, Y. Xie, I. Trojan, S. Medvedev, A. O. Lyakhov, M. Valle and V. Prakapenka, *Nature*, 2009, **458**, 182.
19 J. Zhang, C. Liu, X. Zhang, F. Ke, Y. Han, G. Peng, Y. Ma and C. Gao, *Appl. Phys. Lett.*, 2013, **103**, 052102.
20 C. Berglund and A. Jayaraman, *Phys. Rev.*, 1969, **185**, 1034.
21 E. Arcangeletti, L. Baldassarre, D. Di Castro, S. Lupi, L. Malavasi, C. Marini, A. Perucchi and P. Postorino, *Phys. Rev. Lett.*, 2007, **98**, 196406.
22 C. Marini, E. Arcangeletti, D. Di Castro, L. Baldassare, A. Perucchi, S. Lupi, L. Malavasi, L. Boeri, E. Pomjakushina, K. Conder and P. Postorino, *Phys. Rev. B: Condens. Matter Mater. Phys.*, 2008, **77**, 235111.
23 M. Mitrano, B. Maroni, C. Marini, M. Hanfland, B. Joseph, P. Postorino and L. Malavasi, *Phys. Rev. B: Condens. Matter Mater. Phys.*, 2012, **85**, 184108.
24 C. Gao, Y. Han, Y. Ma, A. White, H. Liu, J. Luo, M. Li, C. He, A. Hao, X. Huang, Y. Pan and G. Zou, *Rev. Sci. Instrum.*, 2005, **76**, 083912.
25 M. Li, C. Gao, Y. Ma, Y. Li, X. Li, H. Li and J. liu, *Rev. Sci. Instrum.*, 2006, **77**, 123902.
26 M. Li, C. Gao, Y. Ma, D. Wang, Y. Li and J. Liu, *Appl. Phys. Lett.*, 2007, **90**, 113507.
27 L. J. v. d. Pauw, *Philips Res. Rep.*, 1958, **13**, 1.
28 L. Bai, Q. Li, S. A. Corr, Y. Meng, C. Park, S. V. Sinogeikin, C. Ko, J. Wu and G. Shen, *Phys. Rev. B: Condens. Matter Mater. Phys.*, 2015, **91**, 104110.
29 A. Y. Mollaev, I. K. Kamilov, R. K. Arslanov, U. Z. Zalibekov, S. F. Marenkin, V. M. Novotortsev and S. A. Varnavskiy, *High Pressure Res.*, 2006, **26**, 387.

This journal is © The Royal Society of Chemistry 2015

30 C. Liu, Y. Sui, W. Ren, B. Ma, Y. Li, N. Su, Q. Wang, Y. Qiang Li, J. Zhang, Y. Han, Y. Ma and C. Gao, *Inorg. Chem.*, 2012, **51**, 7001.
31 C. Chen, Y. Zhao, X. Pan, V. Kuryatkov, A. Bernussi, M. Holtz and Z. Fan, *J. Appl. Phys.*, 2011, **110**, 023707.
32 E. O. Kane, in *Semiconductors and Semimetals*, ed. R. K. Willardson and C. B. Albert, 1966, vol. 1, p. 75.
33 D. Errandonea, A. Segura, D. Martínez-García and V. Muñoz-San Jose, *Phys. Rev. B: Condens. Matter Mater. Phys.*, 2009, **79**, 125203.